Nonlinear Dyn (2024) 112:9445–9458
https://doi.org/10.1007/s11071-024-09508-9

RESEARCH

Spatiotemporally modulated similaritons and composite waves in inhomogeneous system

Kui Huo · Jing Chen · Heping Jia · Rongcao Yang

Received: 4 February 2024 / Accepted: 8 March 2024 / Published online: 12 April 2024

Abstract General and refined spatiotemporal similariton solutions are presented by introducing arbitrary real temporal and spatial modulation functions that construct flexible and controllable relationships among dispersion, nonlinearity and external potential in spatiotemporal modulation inhomogeneous system. The modulated bright similariton (MBS), modulated dark similariton (MDS) and modulated plane wave (MPW) solutions are achieved by a general self-similar transformation method, and modulated dynamics of the MBS, MDS and MPW by choosing Gaussian/periodic temporal function and periodic spatial function. Furthermore, by applying self-similar transformation to M-component spatiotemporal inhomogeneous nonlinear Schrödinger equations, M-component spatiotemporal solutions are obtained and the spatiotemporal modulated properties of 2-component composite waves are studied in detail. The presented results may open many new possibilities for generation and controlling of solitons.

K. Huo · J. Chen · H. Jia · R. Yang (✉)
School of Physics and Electronic Engineering, Shanxi University, Taiyuan 030006, China
e-mail: sxdxyrc@sxu.edu.cn

R. Yang
Collaborative Innovation Center of Extreme Optics, Shanxi University, Taiyuan 03006, China

Keywords Spatiotemporal modulation · Similariton · Composite waves · Inhomogeneous system

1 Introduction

Controllable solitons in inhomogeneous system, which can exist under some constraint relationships among group-velocity dispersion (GVD), nonlinearity and external potential [1–6], have been investigated in the frame of inhomogeneous Gross-Pitaevskii (GP) or nonlinear Schrödinger (NLS) equations. Some analytic methods, such as Darboux transformations [7, 8], Hirota bilinearizations [9, 10], neural networks [11, 12] and self-similar transformations [3, 4, 13–21], have been utilized to find different families of soliton solutions including bright, dark, kink, and gray solitons [13, 22, 23], breathers [7], Peregrine (or rogue waves) [14, 16, 24–26], vortex solitons [27], composite solitary waves [15, 20, 28], dark-bright solitons [17] and vector solitons [29]. These analytical solutions have been applied to investigate matter waves in Bose–Einstein condensates (BEC) [2, 30] and optical solitons in nonlinear optical systems [13, 14]. The amplitudes, trajectories and spectrum of solitons are variously modulated in spatial [1, 2, 7, 13, 15–19], temporal [14, 20, 22, 24, 27–29, 31] and spatiotemporal [3, 4, 21, 23, 25, 32] inhomogeneous systems, and self-similar soliton (i.e. similariton) evolutions have been experimentally observed in nonlinear fiber [33, 34].

In recent years, various solitons have been studied in inhomogeneous system [5, 7–9, 13–17, 21, 22, 25, 28, 31, 35–38]. Tiofack et al. analyzed periodic modulation Kuznetsov-Ma soliton whose shape and position are controlled both by the intensity and frequency of the modulation [35]. Zhong et al. investigated controllable optical rogue waves via temporal [28, 31], spatial [39] and spatiotemporal [36] modulations. Juan et al. constructed resonant, periodically or quasi-periodically oscillating solitons depending on potentials and nonlinearities in spatiotemporal coordinates [3]. Liu et al. studied exact rogue wave solutions on Gaussian [20] and bright soliton backgrounds [37].

Motivated by these works, we construct more *general* and *refined* spatiotemporal similariton solutions including modulated bright similariton (MBS), modulated dark similariton (MDS) and modulated plane wave (MPW) through a new self-similar transformation that can be used to establish the relationship between spatiotemporal inhomogeneous nonlinear Schrödinger (inNLS) equation and NLS equation. Furthermore, we apply the self-similar transformation to M-component spatiotemporal inNLS equations and discuss spatiotemporal modulation properties of the composite waves by classifying the parameters of the wave number and the frequency shift when $M = 2$ in detail. The results presented here may provide new possibilities for control and generation of similaritons in inhomogeneous nonlinear systems.

The analysis presented in this paper is organized as follows. In Sect. 2, we derive more *general* and *refined* exact similariton solutions of the spatiotemporal inNLS equation through a new self-similar transformation. In Sect. 3, based on the introduced arbitrary real Gaussian/periodic temporal modulation function and periodic spatial modulation function, rich dynamics of similaritons in spatiotemporal inhomogeneous systems are demonstrated in detail. In Sect. 4, the spatiotemporal M-component spatiotemporal inNLS equations are investigated and the spatiotemporal modulation properties of the composite waves for the case of $M = 2$ are studied in detail. In Sect. 5, we draw a conclusion with some discussions of our results.

2 Exact similariton solutions of spatiotemporal inNLS system

The homogeneous GP or NLS equations support rich nonlinear wave solutions, such as bright, dark, breathers [7], and rogue waves [14, 26], and so on [15, 17, 27], which are employed to investigate the dynamics of nonlinear waves. For the control of nonlinear waves in time and/or space domain in complex nonlinear physical system [1, 3, 28], the propagation of nonlinear waves can be governed by the following inNLS equation with spatiotemporal modulated coefficients [3, 36]:

$$i\frac{\partial Q}{\partial z} + \delta d(z,t)\frac{\partial^2 Q}{\partial t^2} + \xi r(z,t)|Q|^2 Q + V(z,t)Q = 0. \tag{1}$$

Here, $Q \equiv Q(z, t)$ represents complex wave envelope of electric fields, and z and t represent the spatial and temporal coordinates, respectively. The real spatiotemporal functions $d(z, t)$, $r(z, t)$ and $V(z, t)$ as well as real constants δ and ξ describe the GVD, nonlinearity and external potential, respectively. Equation (1) is also used to model the dynamics of matter waves in BEC [5], where z and t represent normalized time and spatial coordinates, respectively. Correspondingly, the functions $d(z, t)$, $r(z, t)$ and $V(z, t)$ are effective mass of the condensate, strength management of atoms and trapping potential, respectively. Recently, special solutions of Eq. (1) have been found under some special cases of the spatiotemporal constraints in spatiotemporal inhomogeneous systems [3, 4, 21, 23, 25, 32, 36]. Here, we focus on seeking for more *general* exact self-similar solutions of Eq. (1) by introducing a new self-similar transformation for exploring the abundant evolutions of spatiotemporally modulated similaritons and composite waves in inhomogeneous systems.

2.1 Self-similar transformation

To construct more *general* and *refined* similariton solutions of spatiotemporal inNLS equation, we introduce a self-similar transformation

$$Q(z,t) = B(z,t)q\left[Z(z) = \int f(z)dz, T(t) = \int g(t)dt\right], \tag{2}$$

where $Z(z)$ and $T(t)$ are the effective propagation distance and self-similar time variable, $B(z, t)$, $f(z)$ and $g(t)$ are the introduced real functions, respectively. Substituting Eq. (2) into Eq. (1) and applying the conditions $B(z, t) = A(t)$ and $g(t) = 1/A^2(t)$, where $A(t)$ is arbitrary non-zero real function, Eq. (1) can be reduced to the standard NLS Eq. (3):

$$i\frac{\partial q(Z,T)}{\partial Z} + \delta\frac{\partial^2 q(Z,T)}{\partial T^2} + \xi|q(Z,T)|^2 q(Z,T) = 0, \tag{3}$$

where $Z \equiv Z(z)$ and $T \equiv T(t)$. Equation (3) describes the evolutions of various nonlinear waves in optics [40, 41], plasma [42] and hydrodynamics [43, 44] and so on [45, 46]. Meanwhile, the coefficients of GVD, nonlinearity and external potential in Eq. (1) should satisfy the following constraint conditions:

$$d(z,t) = f(z)A^4(t), \tag{4}$$

$$r(z,t) = f(z)/A^2(t), \tag{5}$$

$$V(z,t) = -\delta f(z)A^3(t)A_{tt}(t). \tag{6}$$

To ensure that these conditions have actual physical significance, the introduced function $f(z)$ cannot be zero. In particular, when $A(t)$ and $f(z)$ are non-zero constants, the spatiotemporal inNLS Eq. (1) can degenerate to the standard NLS Eq. (3). Since $A(t)$ and $f(z)$ are *arbitrary* non-zero real functions, the self-similar transformation (2) is a more general one that can degenerate to the previously reported ones in Refs. [14, 20, 24, 28, 31, 35, 37, 47, 48]. For example, if setting $A(t)$ in Gaussian form, i.e. $A(t) = \exp(-t^2/2b^2)$, $f(z) = 1$ and $\delta = 1/2$, $\xi = 1$, according to Eqs. (2), (4)–(6), the two self-similar variables $Z(z)$ and $T(t)$ have the forms of $Z(z) = \int f(z)dz = z$, $T(t) = \int 1/A^2(t)dt = b\pi^{1/2}\mathrm{Erfi}(t/b)/2$, where $\mathrm{Erfi}(\cdot)$ is imaginary error function, and the GVD, nonlinearity and external potential take the forms $d(z, t) = d(t) = \exp(-2t^2/b^2)$, $r(z, t) = r(t) = \exp(t^2/b^2)$ and $V(z, t) = V(t) = (b^2-t^2)\exp(-2t^2/b^2)/(2b^4)$, which are the same with those in Ref. [24]. In Refs. [28, 31], its potential $V(z, t)$ is only the function of variable t in the form of $V(t) = d(t)(a_v t^2 + b_v)$, and $A(t)$ satisfies the equation $A(t)_{tt} + (a_v t^2 + b_v)A(t) = 0$ under $\delta = 1$, $\xi = 2$, $a_v = -1/4$ and $b_v = n + 1/2$, where n is a non-negative integer. Then $A(t)_{tt} + (a_v t^2 + b_v)A(t) = 0$ can be transformed into the parabolic cylinder differential equation with a solution $A(t) = \lambda_1[c_1 D_n(t) + c_2 D_{-n-1}(it)]$ [31], where c_1 and c_2 ($c_1c_2 > 0$) are two integration constants and $\lambda_1 = \{1/[(2\pi)^{1/2}n!]\}^{1/2}$ is the normalization constant, or $A(t) = \lambda D_n(t)$ [28], where $\lambda = 1/[(2\pi)^{1/2}n!]$ is the normalization constant. In the above expression, $D_n(t)$ is a parabolic-cylinder function. In order to exhibit the generality of the self-similar transformation (2), we compare it with those reported in references, as shown in Table 1.

2.2 Exact solutions of spatiotemporally modulated similaritons

Combining the self-similar transformation (2) with Eqs. (4)–(6), Eq. (1) can be transformed into the standard NLS Eq. (3) that possesses the solution of $q(Z, T) = h[\chi = T-T_0-v(Z-Z_0)]\exp[i(\omega T - mZ + \phi_0)]$ [49, 50], where ω, m, v are connected with frequency shift, wave number and velocity, T_0, Z_0, ϕ_0 are related to initial time, position and initial phase, respectively. Substituting the solution $q(Z, T)$ into Eq. (3) yields:

$$\left[\frac{\partial h(\chi)}{\partial \chi}\right]^2 = g_1[h(\chi)]^2 + g_2[h(\chi)]^4 + c', \tag{7}$$

$$v = 2\delta\omega,\ g_1 = \frac{\delta\omega^2 - m}{\delta},\ g_2 = -\frac{\xi}{2\delta}, \tag{8}$$

where c' is an integration constant that is different for respective soliton solutions. According to Eq. (7), one can obtain the bright wave solution:

$$h_B(\chi) = \sqrt{\frac{2(\omega^2\delta - m)}{\xi}}\mathrm{Sech}\left(\sqrt{\frac{\omega^2\delta - m}{\delta}}\chi\right),\ c' = 0 \tag{9}$$

where $\omega^2\delta > (<)\ m$, $\delta > (<)\ 0$, $\xi > (<)\ 0$; and the dark solitary wave solution:

$$h_D(\chi) = \sqrt{\frac{\omega^2\delta - m}{\xi}}\mathrm{Tanh}\left(\sqrt{\frac{\omega^2\delta - m}{-2\delta}}\chi\right),\quad c' = \frac{\delta\omega^2 - m}{2\delta\xi}, \tag{10}$$

where $\omega^2\delta > (<)\ m$, $\delta < (>)\ 0$, $\xi > (<)\ 0$; and the plane wave solution:

Table 1 Comparison of the self-similar transformation with previously reported ones

References	$A(t)$	$f(z)$	$Z(z)$	$T(t)$
[37, 48]	$k\mathrm{sech}(kt)$	$f(z)$	$\int f(z)dz$	$t/(2k^2) + \mathrm{Sinh}(2kt)/(4k^3)$
[24]	$\exp(-t^2/2b^2)$	1	z	$b\pi^{1/2}\mathrm{Erfi}(t/b)/2$
[28, 31]	$\lambda_1[c_1D_n(t) + c_2D_{-n-1}(it)]$	1	z	$\int 1/A^2(t)dt$
[14, 20]	$A(t)$	1	z	$\int 1/A^2(t)dt$
[35, 47]	1	$f(z)$	$\int f(z)dz$	t
This work	*arbitrary* real function	*arbitrary* real function	$\int f(z)dz$	$\int 1/A^2(t)dt$

$$h_P(\chi) = \sqrt{\frac{\omega^2\delta - m}{\xi}},\ c' = \frac{\delta\omega^2 - m}{2\delta\xi}, \tag{11}$$

where $\omega^2\delta > (<)\ m$, $\xi > (<)\ 0$.

Then, using the solitary wave solutions (9)–(11) and the inverse process of the self-similar transformation Eq. (2), one can obtain the solutions of modulated bright similariton (MBS), modulated dark similariton (MDS) and modulated plane wave (MPW) solutions for the spatiotemporal inNLS Eq. (1):

MBS solution

$$Q_{MBS} = A(t)\sqrt{\frac{2(\omega^2\delta - m)}{\xi}}\mathrm{Sech}\left\{\sqrt{\frac{\omega^2\delta - m}{\delta}}\left[\int 1/A^2(t)dt - T_0 - 2\delta\omega\left(\int f(z)dz - Z_0\right)\right]\right\}e^{i\left[\omega\int 1/A^2(t)dt - m\int f(z)dz + \phi_0\right]}, \tag{12}$$

MDS solution

$$Q_{MDS} = A(t)\sqrt{\frac{\omega^2\delta - m}{\xi}}\mathrm{Tanh}\left\{\sqrt{\frac{\omega^2\delta - m}{-2\delta}}\left[\int 1/A^2(t)dt - T_0 - 2\delta\omega\left(\int f(z)dz - Z_0\right)\right]\right\}e^{i\left[\omega\int 1/A^2(t)dt - m\int f(z)dz + \phi_0\right]}, \tag{13}$$

MPW solution

$$Q_{MPW} = A(t)\sqrt{\frac{\omega^2\delta - m}{\xi}}e^{i\left[\omega\int 1/A^2(t)dt - m\int f(z)dz + \phi_0\right]}. \tag{14}$$

It is obviously to see from Eqs. (12)–(14) that the temporal modulation function $A(t)$ is related to the amplitude and chirp parameters and the spatial modulation function $f(z)$ is associated with the trajectory and phase. Also, according to Eqs. (12)–(14), the amplitudes and shapes of MBS, MDS and MPW can be arbitrarily modulated by the $A(t)$. What is more, the intensity of Q_{MPW} is independent of $f(z)$. Thus, Eq. (14) can be used to describe exact bright and dark (gray) soliton trains when setting $A(t) = \rho_0 + \rho_1\mathrm{Sech}[\eta_1(t-t_1)] + \rho_2\mathrm{Sech}[\eta_2(t-t_2)] + \cdots + \rho_n\mathrm{Sech}[\eta_n(t-t_n)]$ and $A(t) = \rho_0 + \rho_1\mathrm{Tanh}^2[\eta_1(t-t_1)] + \rho_2\mathrm{Tanh}^2[\eta_2(t-t_2)] + \cdots + \rho_n\mathrm{Tanh}^2[\eta_n(t-t_n)]$, where ρ_n, η_n and t_n ($n = 1, 2, 3, \ldots$) are the amplitude, width and initial position parameters of n-bright and n-dark (gray) solitons by setting $f(z) = 1$. Figure 1 depicts the evolutions of 5-bright soliton and 5-gray soliton (see Fig. 1a and b) and the corresponding profiles of the GVD, nonlinearity and external potential (see Fig. 1c and d) in inhomogeneous system.

In this paper, we focus on the dynamics of MBS, MDS and MPW in spatiotemporal inhomogeneous system under different temporal modulation function $A(t)$ and spatial modulation function $f(z)$. In fact, for special case of $\delta = 1$, $\xi = 2$, there exist abundant solutions to NLS Eq. (3), such as bright solitons [50], Akhmediev breathers and Ma breathers [51], and rogue waves [52], which one can easily obtain their similariton solutions of Eq. (1) through the inverse transformation of Eq. (2).

3 Dynamical behaviors of spatiotemporally modulated similaritons

Since both $A(t)$ and $f(z)$ are *arbitrary* temporal and spatial real functions, the GVD, nonlinearity and external potential are more general according to Eqs. (4)–(6), meaning that spatiotemporal modulation of similaritons can theoretically be realized at will, which opens many new possibilities for generating and controlling similaritons. In this section, we consider the dynamics of MBS, MDS and MPW under typical

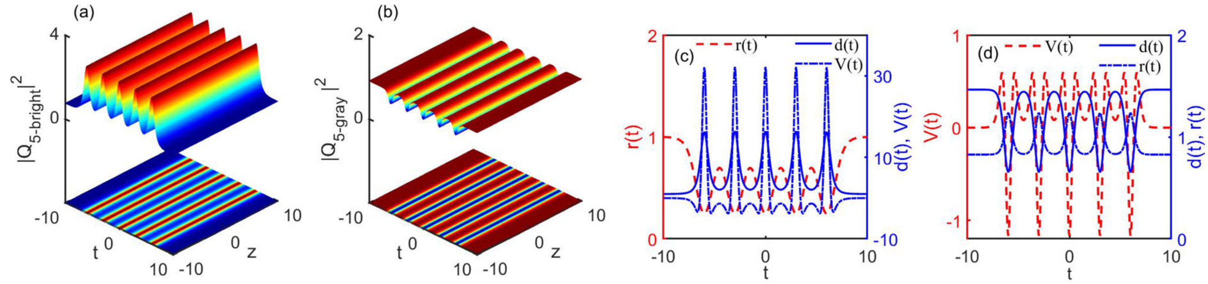

Fig. 1 The evolutions of **a** 5-bright and **b** 5-gray solitons. **c** 5-bright and **d** 5-gray soliton profiles of GVD, nonlinearity and external potential. The adopted 5-bright parameters are $\rho_0 = \rho_1 = \rho_2 = \rho_3 = \rho_4 = \rho_5 = 1$, and 5-gray parameters are $\rho_0 = 0.1$, $\rho_1 = \rho_2 = \rho_3 = \rho_4 = \rho_5 = 0.2$. The other parameters are $t_1 = -6, t_2 = -3, t_3 = 0, t_4 = 3, t_5 = 6$. $\eta_1 = \eta_2 = \eta_3 = \eta_4 = \eta_5 = 2$, respectively

Gaussian/periodic temporal modulation function and periodic spatial modulation function.

3.1 Similaritons with Gaussian-periodic spatiotemporal modulation

The Gaussian temporal modulation function $A(t)$ and the periodic spatial function $f(z)$ are considered as

$$A(t) = b_0 \exp\left(-t^2/b^2\right), f(z) = \eta_{z1} \sin(\varepsilon_{z1} z), \tag{15}$$

where b_0 and b stand for the magnitude and width parameters of Gaussian-shape $A(t)$, η_{z1} and ε_{z1} describe the strength and frequency of the periodic spatial function $f(z)$. In this case, the effective propagation distance and self-similar time have the forms of $Z(z) = -\eta_{z1}\cos(\varepsilon_{z1}z)/\varepsilon_{z1}$ and $T(t) = b(\pi/8)^{1/2}\mathrm{Erfi}[2^{1/2}t/b]b_0^{-2}/2$. According to Eqs. (4)–(6), the spatiotemporal inhomogeneous parameters of GVD, nonlinearity and external potential take the forms of $d(z, t) = \eta_{z1}b_0^4\exp(-4t^2/b^2)\sin(\varepsilon_{z1}z)$, $r(z, t) = \eta_{z1}b_0^{-2}\exp(2t^2/b^2)\sin(\varepsilon_{z1}z)$ and $V(z, t) = 2\delta\eta_{z1}b_0^4\exp(-4t^2/b^2)(b^2-2t^2)\sin(\varepsilon_{z1}z)/b^4$, respectively. Figure 2 presents the dynamics of MBS, MDS and MPW modulated by Gaussian temporal modulation function $A(t)$ and periodic spatial modulation function $f(z)$. As shown in Fig. 2a and d, the evolution trajectories of the MBS and MDS are in a straight line when $\omega = 0$ although $d(z, t)$ and $r(z, t)$ are periodic along the propagation distance. This is in accordance with the solutions of MBS (Eq. 12) and MDS (Eq. 13), i.e. the MBS and MDS have zero velocity when $\omega = 0$. Interestingly, the evolutions of MDS present double solitons due to Gaussian-shape $d(z, t)$ and $r(z, t)$ with wider distributions along the temporal coordinates (see Fig. 2d–f). However, when $\omega \neq 0$, the evolution trajectories of MBS and MDS are periodic because of periodic $d(z, t)$ and $r(z, t)$ along the propagation distance (see Fig. 2b, c and e, f), which can be explained by $\chi = T(t)-T_0-v[Z(z) - Z_0]$, and the evolution trajectory range in temporal coordinate can be modulated by the parameter b (see Fig. 2b, c or e, f). According to Eq. (14), the intensity of MPW is $|Q_{\mathrm{MPW}}|^2 = A^2(t)(\omega^2\delta-m)/\xi$, which indicates that the evolution trajectory of the MPW is independent of the spatial modulation function $f(z)$ while the distribution of MPW is strongly dependent on the temporal modulation function $A(t)$, exhibiting a Gaussian shape in time coordinates (see Fig. 2g, h and i). It is noted that the intensities are different between Fig. 2g and h as the intensity of Q_{MPW} is dependent on ω.

3.2 Similaritons with periodic-periodic spatiotemporal modulation

The temporal modulation function $A(t)$ and spatial modulation function $f(z)$ are considered as

$$A(t) = 1 + 0.5\cos(\varepsilon_A t), f(z) = \eta_{z2} \sin(\varepsilon_{z2} z), \tag{16}$$

where ε_A describes the frequency of periodic fluctuations of the periodic temporal modulation function $A(t)$; and η_{z2} and ε_{z2} describe the strength and frequency of periodic spatial modulation function $f(z)$. In this case, the effective propagation distance and self-similar time have the forms $Z(z) = -\eta_{z2}\cos(\varepsilon_{z2}z)/\varepsilon_{z2}$, $T(t) = 4\{4 \times 3^{1/2}\arctan[\tan(\varepsilon_A t/2)/3^{1/2}][2 + \cos(\varepsilon_A t)] -3\sin(\varepsilon_A t)\}[2 + \cos(\varepsilon_A t)]^{-1}/(9\varepsilon_A)$. According to Eqs. (4)–(6), the spatiotemporal inhomogeneous parameters of GVD, nonlinearity and external potential take the forms of $d(z, t) = \eta_{z1}[1 + 0.5\cos(\varepsilon_A t)]^4\sin(\varepsilon_{z2}z)$, $r(z, t) = \eta_{z2}[1 + 0.5\cos(\varepsilon_A t)]^{-2}\sin(\varepsilon_{z2}z)$ and

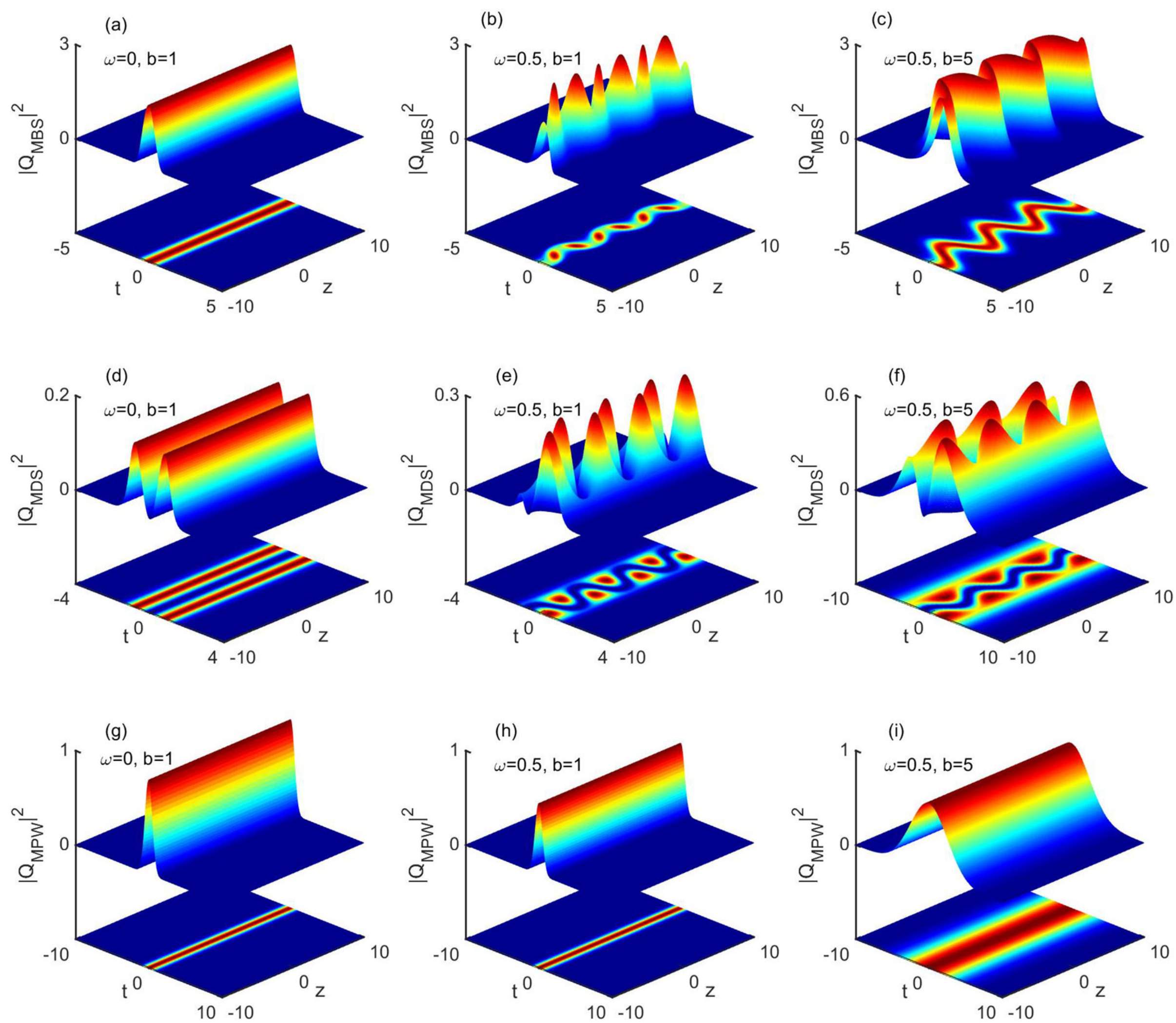

Fig. 2 The evolutions of the **a**–**c** MBS with $m = -1$, $\delta = \xi = 1$; **d**–**f** MDS with $m = -1$, $\delta = -\xi = -1$; **g**–**i** MPW with $m = -1$, $\delta = -\xi = -1$ in the system (15) under Gaussian-periodic spatiotemporal modulation with the parameters **a**, **d**, **g** $b = 1, \omega = 0$, **b**, **e**, **h** $b = 1, \omega = 0.5$, **c**, **f**, **i** $b = 5, \omega = 0.5$. The other parameters are $Z_0 = T_0 = 0$, $\eta_{z1} = 1$, $\varepsilon_{z1} = 1$, $\varphi_0 = 0$, respectively

$V(z, \quad t) = \varepsilon_A{}^2\delta\eta_{z2}\cos(\varepsilon_A t)[2 + \cos(\varepsilon_A t)]^3\sin(\varepsilon_{z2}z)/16$, respectively. Similarly, according to the expressions of MBS and MDS solutions (12) and (13), when $\omega = 0$, the velocities of MBS and MDS are independent of z, leading to a straight propagation (see Fig. 3a and c), while have eriodic profiles about time t due to periodic modulation. However, when $\omega \neq 0$, both MBS and MDS exhibit periodic characteristics both in spatial and temporal coordinates (see Fig. 3b and d). For the MPW, it shows straight transmission along the propagation distance with the periodic distribution in temporal coordinates whether ω is zero or not (see Fig. 3e and f), which can be explained by the MPW solution (14) whose intensity is independent of z, only the phase shift is related the spatial modulation function $f(z)$.

Furthermore, we discuss the stability of the similaritons (12)–(14) with periodic-periodic spatiotemporal modulation by adding 10% random white noise on their background and 10% amplitude fluctuation in the initial pulses. Figure 4a–c and d–f respectively present the numerical results of MBS, MDS and MPW corresponding to above two perturbed ways. By comparing with Fig. 3a, c and e, it is shown that the

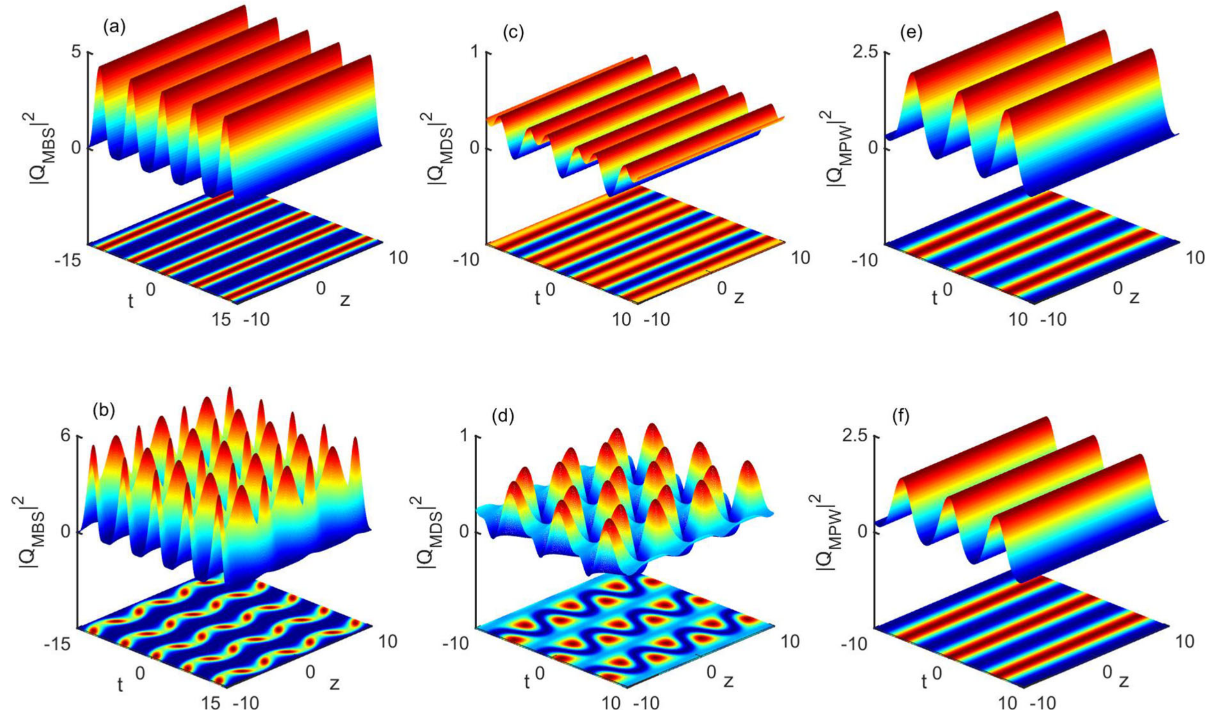

Fig. 3 The evolutions of the **a**, **b** MBS, **c**, **d** MDS and **e**, **f** MPW in the system (16) under periodic-periodic spatiotemporal modulation. The parameters are $\varepsilon_A = 1$, $\eta_{z2} = 1$, $\varepsilon_{z2} = 1$, respectively. The other parameters are the same as Fig. 2a, b, d, e and g, h

MBS, MDS and MPW can propagate in a stable way and keep their main evolution characteristics under the random white noise perturbation and initial amplitude fluctuation.

4 Similaritons of *M*-component spatiotemporal inNLS equations

In this section, we expand and apply the self-similar transformation (2) into *M*-component spatiotemporal inNLS equations and investigate the dynamics of composited similariton waves in inhomogeneous multi-mode fiber which can be described by the following equations [14, 53–55]:

$$i\frac{\partial U_j}{\partial z}+\delta d(z,t)\frac{\partial^2 U_j}{\partial t^2}+\xi r(z,t)\left(a_1\left|U_j\right|^2+a_2\sum_{l=1,l\neq j}^{M}\left|U_l\right|^2\right)U_j +\xi a_3 r(z,t)\sum_{l=1,l\neq j}^{M}U_l^2U_j^*+V(z,t)U_j=0, j=1,\,2,\,...,M, \tag{17}$$

where a_1, a_2 and a_3 represent self-phase modulation, cross-phase modulation and coherent four-wave mixing coupling effects, respectively. Former works have studied some special cases as $M = 2$, $\delta = 1$, $\xi = 2$, $a_1 = 1$, $a_2 = 2$, $a_3 = -2$ in Ref. [14], $M = 2, 3$, $\delta = 1$, $\xi = 2$, $a_1 = a_2 = 2$, $a_3 = 0$ in Ref. [20] and $M = 2$, $\delta = 1$, $\xi = 2$, $a_1 = a_2 = 1$, $a_3 = 0$ in Ref. [28].

In the same way, combining self-similar transformation $U_j(z,\ t) = A(t)u_j[Z(z) = \int f(z)dz,\ \ T(t) = \int 1/A^2(t)dt]$ with Eqs. (4)–(6), we can transform Eq. (17) into *M*-component NLS equations as the following form [14, 56]:

$$i\frac{\partial u_j}{\partial Z}+\delta\frac{\partial^2 u_j}{\partial T^2}+\xi\left(a_1\left|u_j\right|^2+a_2\sum_{l=1,l\neq j}^{M}\left|u_l\right|^2\right)u_j + \xi a_3\sum_{l=1,l\neq j}^{M}u_l^2u_j^*=0, j=1,\,2,\,...,M. \tag{18}$$

Theoretically, we can investigate the spatiotemporal modulation of similaritons in *M*-component spatiotemporal system based on the above self-similar transformation and the solutions of Eq. (18). To our knowledge, even the case of $M = 2$, $a_1 = 1$, $a_2 = 2$,

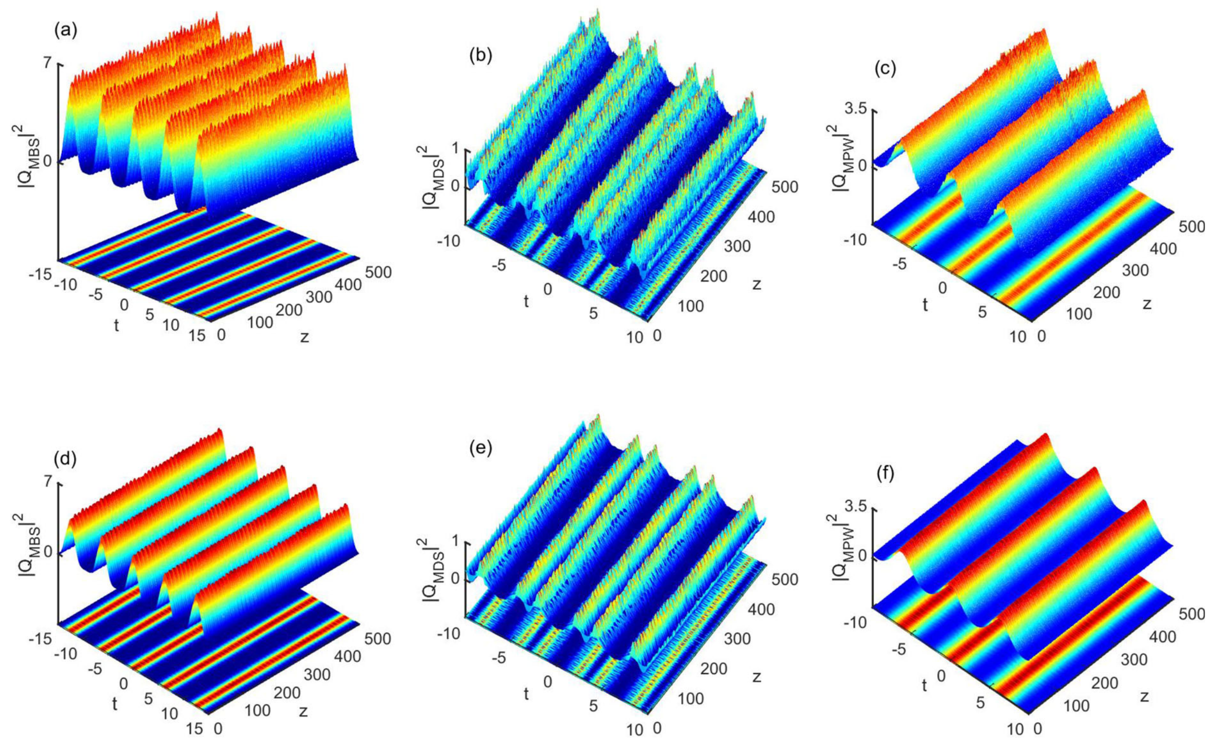

Fig. 4 The numerical evolution of **a**, **d** MBS, **b**, **e** MDS and **c**, **f** MPW by adding 10% random white noise (top row) and 10% amplitude fluctuation. The other adopted parameters are the same as in Fig. 3a, c and e, respectively

and $a_3 = 1$ has not been addressed before. For simplicity, here we consider the 2-component spatiotemporal system. Using the assumption $u_1 = (q_1 + q_2)/2$ and $u_2 = (q_1 - q_2)/2$ [15, 57], Eq. (18) can be decoupled to $iq_{jZ} + \delta q_{jTT} + \xi|q_j|^2 q_j = 0$, where $j = 1, 2$, which has the same form as Eq. (3). So the solutions of 2-component spatiotemporal inNLS equations are

$$U_j = \frac{A(t)}{2}\left\{h_1\left[\chi = \int 1/A(t)^2 dt - T_{01} - v_1\left(\int f(z)dz - Z_{01}\right)\right] e^{i\left[\omega_1 \int 1/A^2(t)dt - m_1 \int f(z)dz + \phi_{01}\right]} - (-1)^j h_2\left[\chi = \int 1/A(t)^2 dt - T_{02} - v_2\left(\int f(z)dz - Z_{02}\right)\right] e^{i\left[\omega_2 \int 1/A^2(t)dt - m_2 \int f(z)dz + \phi_{02}\right]}\right\}, j = 1, 2. \tag{19}$$

where $h_j[\chi]$ ($j = 1, 2$) is one of the solutions (9)–(11). The 2-component solutions (19) imply that there exist a variety of highly-controllable composite waves in the inhomogeneous fiber systems due to arbitrary temporal modulation function $A(t)$ and spatial modulation function $f(z)$, although the parameters of GVD, nonlinearity and external potential relationships need to satisfy Eqs. (4)–(6). Combining Eq. (19) and the solutions (9)–(14) with the existence conditions, MBS–MDS composite waves are not supported due to their incompatible parameters δ and ξ for MBS and MDS, then five kinds of composite waves, such as MBS–MBS, MDS–MDS, MPW–MPW, MBS–MPW, MDS–MPW, in 2-component inhomogeneous system with spatiotemporal modulation can be obtained. Here only MDS–MDS, MPW–MPW and MDS–MPW composite waves are investigated as examples, other two composite waves may be discussed if readers are interested.

The considered temporal modulation function $A(t)$ and spatial modulation function $f(z)$ are the same as Eq. (15), and the corresponding parameters of GVD, nonlinearity and external potential relationships can be obtained according to Eqs. (4)–(6). For the convenience of discussion, we classify spatiotemporal modulation properties of the composite waves by the parameters of the wave number m and the frequency shift ω.

Case 1: When $\omega_1 = \omega_2 = 0$ and $m_1 = m_2 = m$, according to Eq. (19), the intensities of MDS–MDS, MPW–MPW, and MDS–MPW are presented as follows:

$$\left|U_j\right|^2 = A^2(t)\left[h_1^2(\chi) + h_2^2(\chi) - (-1)^j 2h_1(\chi)h_2(\chi)\cos(\phi_{02} - \phi_{01})\right]/4, j = 1, 2, \tag{20}$$

where $h_j(\chi) = h_j[\chi = \int 1/A^2(t)dt - T_{0j}]$. It is obvious to see from Eq. (20) that the intensities of $|U_j|^2$ are independent of the spatial modulation function $f(z)$, resulting in that the composite waves in this case are not spatially modulated. In general, two components of the composite waves (20) have different intensities, i.e. $|U_1|^2 \neq |U_2|^2$. For example, when $\phi_{01} - \phi_{02} = l\pi$, where l is an integer, the intensity of the MDS–MDS wave is $|U_{j\text{MDS–MDS}}|^2 = A^2(t)|m/(4\xi)|\{\text{Tanh}[(m/2\delta)^{1/2}\chi_1] - (-1)^{j+l}\text{Tanh}[(m/2\delta)^{1/2}\chi_2]\}^2$, where $\chi_j = \int 1/A^2(t)dt - T_{0j}$ (j = 1,2), and its two components respectively exhibit double-peak bright soltion and single-peak bright soliton due to the Gaussian-shape $d(z, t)$ and $r(z, t)$ modulation, as shown in Fig. 5a. When $\phi_{01} - \phi_{02} \neq l\pi$, the intensity of MPW–MPW is $|U_{j\text{MPW–MPW}}|^2 = A^2(t)|m/(2\xi)|[1 - (-1)^j\cos(\phi_{01} - \phi_{02})]$ and its two components show bright and bright waves because of Gaussian-shape temporal modulation function $A(t)$ in Fig. 5b. For MDS–MPW composite wave, its intensity is $|U_{j\text{MDS–MPW}}|^2 = A^2(t)|m/(2\xi)|\{1 + \text{Tanh}^2[(m/2\delta)^{1/2}\chi] - (-1)^j 2\text{Tanh}[(m/2\delta)^{1/2}\chi]\cos(\phi_{02} - \phi_{01})\}$, showing right-soliton (Fig. 5c1) and left-soliton (Fig. 5c2). It should be note that when $\phi_{01} - \phi_{02} = (2l + 1)\pi/2$, two components of the composite waves (20) have the same intensities, i.e., $|U_1|^2 = |U_2|^2$, which are not presented here.

Case 2: When $\omega_1 = \omega_2 \neq 0$, $m_1 = m_2 = m$, and $v \neq 0$. Then, the intensities of the composite waves have the same form as that in Eq. (20) except $h_j = h_j[\chi = \int 1/A^2(t)dt - T_{0j} - v(\int f(z)dz - Z_{0j})]$. This means that in this case, the composite waves (19) can be spatially and temporally modulated except for the MPW–MPW because the MPW is independent of v according to the solution of Eq. (14). As the evolution of the MPW–MPW is only in intensity different from Fig. 5b according to Eqs. (14) and (19), we do not present it here. Interesting, the evolution of the MDS–MDS appears zipper-like and snake-like forms shown in Fig. 6a, while the evolution of the MDS–MPW shows right-zipper and left-zipper form in Fig. 6b. Moreover, these evolutions of both MDS–MDS and MDS–MPW are periodic along with the propagation distance and localized in temporal coordinates in Figs. 6a and 5b because of periodic $f(z)$ and Gaussian-shape $A(t)$, respectively.

Case 3: When $\omega_1 \neq \omega_2$ and $m_1 = m_2 = m$, the intensities of components of the composite waves can be written as the following forms:

$$\left|U_j\right|^2 = A^2(t)\left\{h_1^2 + h_2^2 - (-1)^j 2h_1h_2\cos\left[(\omega_2 - \omega_1)\int A(t)^{-2}dt + (\phi_{02} - \phi_{01})\right]\right\}/4, j = 1, 2. \tag{21}$$

When $\omega_1 \neq \omega_2$, the evolutions of MDS–MDS, MPW–MPW and MDS–MPW are multi-peak in temporal as shown in Fig. 7a, b and c, which can be explained by the term $h_1h_2\cos[(\omega_2 - \omega_1)\int 1/A^2(t)dt + (\phi_{02} - \phi_{01})]$ in Eq. (21). Moreover, the intensity evolutions of MDS–MDS and MDS–MPW are more interestingly modulated in spatial coordinates due to $\chi = \int 1/A^2(t)dt - T_0 - v(\int f(z)dz - Z_0)$. While, the intensity evolution of MPW–MPW is not modulated in spatial coordinates because of the intensity of MPW is independent of periodic $f(z)$ according to Eq. (14).

Case 4: When $\omega_1 = \omega_2 = \omega$, $m_1 \neq m_2$, the intensities of components of the composite waves can be written as the following forms:

$$\left|U_j\right|^2 = A^2(t)\left\{h_1^2 + h_2^2 - (-1)^j 2h_1h_2\cos\left[(m_1 - m_2)\int f(z)dz + (\phi_{02} - \phi_{01})\right]\right\}/4, j = 1, 2. \tag{22}$$

In this case, the evolutions of MDS–MDS, MPW–MPW and MDS–MPW are periodic in spatial coordinates due to the existing term $h_1h_2\cos[(m_1 - m_2)\int f(z)dz + (\phi_{02} - \phi_{01})]$ in Eq. (22). When $\omega = 0$, the trajectory evolutions of MDS–MDS and MDS–MPW are independent of periodic spatial modulation function $f(z)$ as shown in Fig. 8a and c by reason of $h_j = h_j[\chi = \int 1/A^2(t)dt - T_{0j}]$. On the other hand, when $\omega \neq 0$, i.e. $v \neq 0$, the intensity evolutions of MDS–MDS and MDS–MPW are related to periodic spatial modulation function $f(z)$ as shown in Fig. 8d and f by reason of $h_j = h_j[\chi = \int 1/A^2(t)dt - T_{0j} - v(\int f(z)dz - Z_{0j})]$. In addition, whether ω are equal to zero or not, the evolutions of composite waves are periodic in spatial coordinates due to the term $(m_1 - m_2)\int f(z)dz$ in Eq. (22),

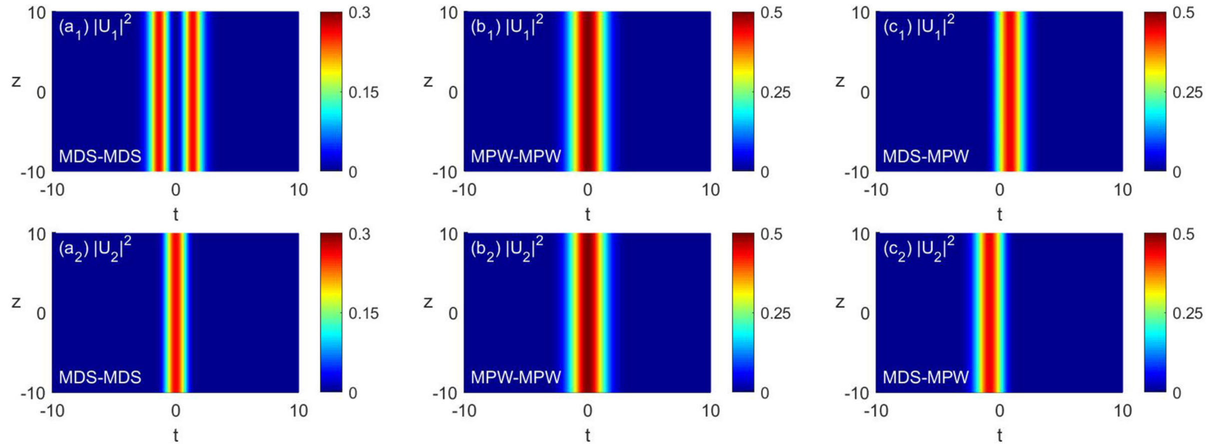

Fig. 5 The evolutions of the composite waves **a** MDS–MDS, **b** MPW–MPW, **c** MDS–MPW in the system (15) for Case 1. The corresponding parameters of MDS and MPW are the same as in Fig. 2d and h, and the other parameters are **a** $\varphi_{02} = 0$, $T_{01} = -T_{02} = 0.8$, $Z_{01} = Z_{02} = 0$, **b** $\varphi_{02} = \pi/2$, $T_{01} = T_{02} = 0$, $Z_{01} = Z_{02} = 0$, **c** $\varphi_{02} = 0$, $T_{01} = T_{02} = 0$, $Z_{01} = Z_{02} = 0$, respectively

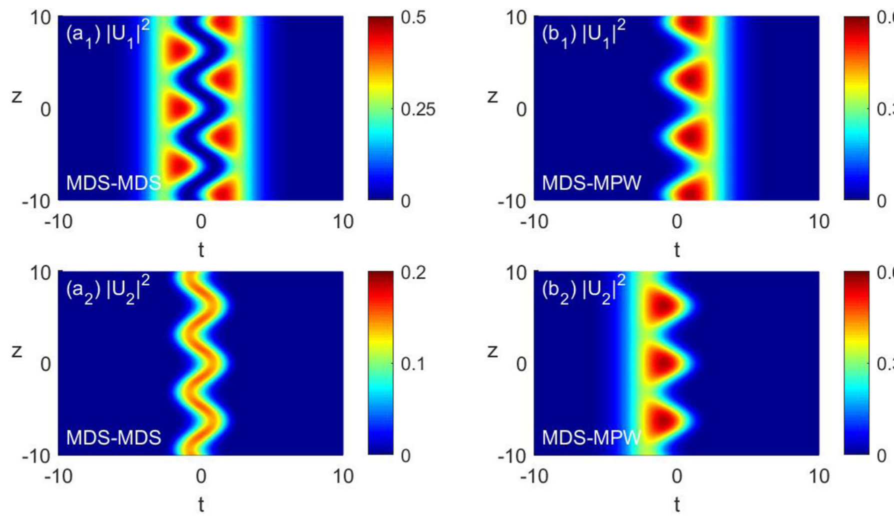

Fig. 6 The evolutions of the composite waves **a** MDS–MDS, **b** MDS–MPW in system (15) for Case 2. The corresponding parameters are the same as in Fig. 5a, c, except for $b = 4$, $\omega_1 = \omega_2 = 0.5$

but the dynamics of MPW–MPW is always travels along the same path because of $h[\chi]$ which is independent of periodic spatial modulation $f(z)$ according to Eqs. (14) and (22) and the intensities are different due to the term $h_{Pj} = [(\omega^2\delta - m_j)/\xi]^{1/2}$ in Eq. (22) as shown in Fig. 8b and e.

Case 5: When $\omega_1 \neq \omega_2$, $m_1 \neq m_2$, the intensities of components of the composite waves can be written as the following forms:

$$|U_j|^2 = A^2(t)\left\{h_1^2 + h_2^2 - (-1)^j 2h_1h_2\cos\left[(\omega_2-\omega_1)\int 1/A(t)^2dt + (m_1-m_2)\int f(z)dz + (\phi_{02}-\phi_{01})\right]\right\}/4, j = 1, 2. \tag{23}$$

In this case, the intensity evolutions of MDS–MDS, MPW–MPW and MDS–MPW are periodic in spatial and multi-peak in temporal coordinates as shown in Fig. 9 because of the term $(m_1 - m_2)\int f(z)dz$ and $(\omega_2 - \omega_1)\int 1/A^2(t)dt$ in Eq. (23), respectively. The periodic evolution trajectories of MDS–MDS, MPW–MPW and MDS–MPW can be ducuced by $h_j = h_j[\chi = \int 1/A^2(t)dt - T_{0j} - v(\int f(z)dz - Z_{0j})]$ where $f(z)$ is periodic along the propagation distance. Interestingly, the intensity evolutions of MDS–MDS and MDS–MPW (Fig. 9a and c) are more complex than others cases due to the term $h_1h_2\cos[(\omega_2 - \omega_1)\int 1/A^2(t)dt + (m_1 - m_2)\int f(z)dz + (\phi_{02} - \phi_{01})]$.

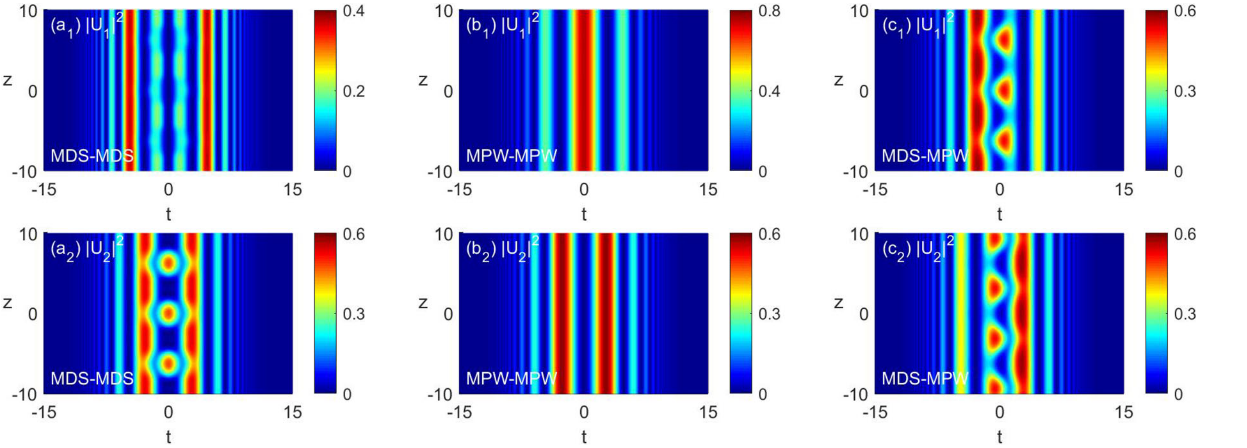

Fig. 7 The evolutions of composite waves **a** MDS–MDS, **b** MPW–MPW, **c** MDS–MPW in the system (15) for Case 3. The corresponding parameters are the same as in Fig. 5, except for $b = 8$, $\omega_1 = -\omega_2 = -0.5$

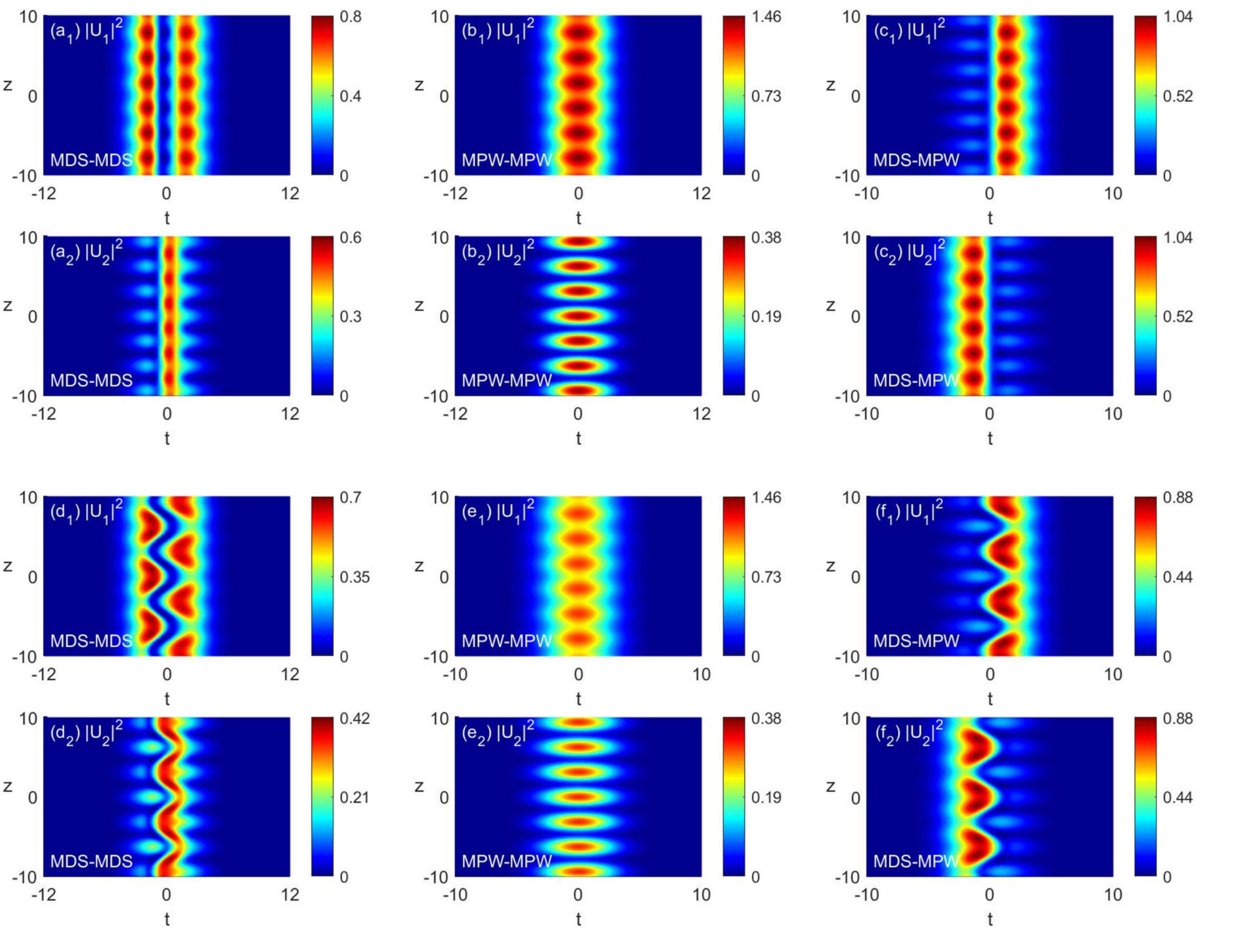

Fig. 8 The evolutions of composite waves **a**, **d** MDS–MDS, **b**, **e** MPW–MPW, **c**, **f** MDS–MPW in the system (15) for Case 4. The corresponding parameters are the same as in Fig. 7, except for $b = 4$, $m_1 = -2$, $m_2 = -1$, **a**–**c** $\omega = 0$, **d**–**f** $\omega = 0.5$

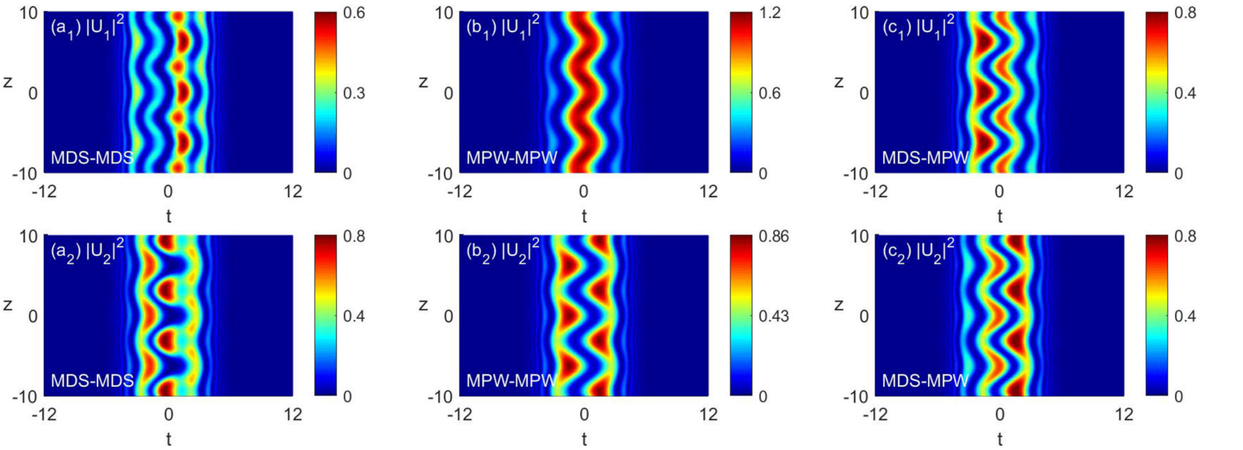

Fig. 9 The evolutions of the composite waves **a** MDS–MDS, **b** MPW–MPW, **c** MDS–MPW in the system (15) for Case 5. The corresponding parameters are the same as those in Fig. 7 except for $m_1 = -2$, $m_2 = -1$

5 Conclusion and discussion

In this work, we have reported more general and refined similariton solutions including MBS, MDS and MPW, and established the relationship between spatiotemporal inNLS equation and NLS equation by a new self-similar transformation method. What is more, the more flexible and controllable relationships among dispersion, nonlinearity and external potential are constructed by introducing arbitrary temporal and spatial modulation functions. To demonstrate the spatiotemporal modulation properties, we investigated the dynamics of MBS, MDS and MPW with Gaussian/periodic temporal modulation and periodic spatial modulation. Furthermore, we discussed the stability of MBS, MDS and MPW in periodic-periodic spatiotemporal modulation system under 10% random white noise perturbation and 10% initial amplitude fluctuation. The numerical results show that the similaritons can keep stable evolutions after propagating 500 dispersion lengths. The reported various solitons with infinite-width background may raise the experiment and potential application possibility in nonlinear optics under the Gaussian-shape temporal modulation function [24, 58], and the periodic similaritons in temporal coordinates are easily obtained by periodic-shape temporal modulation function $A(t)$ modulation [14, 20].

The self-similar transformation reported in this work has been applicable for studying M-component spatiotemporal inNLS systems. As example, we studied the case of $M = 2$ and classified spatiotemporal modulation properties of the composite waves by the wave number m and frequency shift ω parameters, which have shown the rich modulations. For the case of multi-component ($M \geq 2$) wave interaction, it maybe involve some novel and interesting dynamics, which will be investigated in the future. Our work may open many new possibilities for generation and controlling similaritons. Moreover, the general and refined solutions benefit the theoretical studies and respective experimental realization in spatiotemporal inNLS and M-component spatiotemporal inNLS systems.

Author contribution Kui Huo: Methodology, Software, Data analysis, Writing-original draft. Jing Chen: Writing-review & editing. Heping Jia: Writing-review & editing. Rongcao Yang: Conceptualization, Theoretical analysis, Supervision.

Funding This work was supported by the National Natural Science Foundation of China (Grant no: 62305199) and the Natural Science Foundation of Shanxi Province (Grant no: 202203021221016).

Data availability Our manuscript has no associated data.

Declarations

Competing interests The authors have no relevant financial or non-financial interests to disclose.

References

1. Serkin, V.N., Hasegawa, A., Belyaeva, T.L.: Nonautonomous solitons in external potentials. Phys. Rev. Lett. **98**, 074102 (2007)
2. Kengne, E., Liu, W.M.: Management of matter-wave solitons in Bose-Einstein condensates with time-dependent atomic scattering length in a time-dependent parabolic complex potential. Phys. Rev. E **98**, 012204 (2018)
3. Juan, B.B., Víctor, M.P.G., Vadym, V., Vladimir, V.K.: Localized nonlinear waves in systems with time- and space-modulated nonlinearities. Phys. Rev. Lett. **100**, 164102 (2008)
4. Chen, S.H., Dudley, J.M.: Spatiotemporal nonlinear optical self-similarity in three dimensions. Phys. Rev. Lett. **102**, 233903 (2009)
5. Kengne, E., Liu, W.M., Malomed, B.A.: Spatiotemporal engineering of matter-wave solitons in Bose-Einstein condensates. Phys. Rep. **899**, 1–62 (2021)
6. Huo, K., Yang, R.C., Jia, H.P., He, Y.J., Christian, M.: Exact similariton solution families and diverse composite waves in coherently coupled inhomogeneous systems. Nonlinear Dyn. **111**, 14435–14451 (2023)
7. Yang, D.Y., Tian, B., Wang, M., Zhao, X., Shan, W.R., Jiang, Y.: Lax pair, Darboux transformation, breathers and rogue waves of an N-coupled nonautonomous nonlinear Schrödinger system for an optical fiber or a plasma. Nonlinear Dyn. **107**, 2657–2666 (2022)
8. Ding, C.C., Gao, Y.T., Deng, G.F., Wang, D.: Lax pair, conservation laws, Darboux transformation, breathers and rogue waves for the coupled nonautonomous nonlinear Schrödinger system in an inhomogeneous plasma. Chaos Solitons Fractals **133**, 109580 (2020)
9. Yang, R.C., Gao, J., Jia, H.P., Tian, J.P., Christian, J.M.: Ultrashort nonautonomous similariton solutions and the cascade tunneling of interacting similaritons. Opt. Commun. **459**, 125025 (2020)
10. Chen, H.Y., Zhu, H.P.: Higher-dimensional vector two-component solitons of a nonautonomous partially nonlocal coupled NLS model in a linear and harmonic potential. Nonlinear Dyn. **111**, 581–590 (2023)
11. Wen, X.K., Jiang, J.H., Liu, W., Dai, C.Q.: Abundant vector soliton prediction and model parameter discovery of the coupled mixed derivative nonlinear Schrödinger equation. Nonlinear Dyn. **111**, 13343–13355 (2023)
12. Xu, S.Y., Zhou, Q., Liu, W.: Prediction of soliton evolution and equation parameters for NLS–MB equation based on the phPINN algorithm. Nonlinear Dyn. **111**, 18401–18417 (2023)
13. Triki, H., Kruglov, V.I.: Chirped self-similar solitary waves in optical fibers governed with self-frequency shift and varying parameters. Chaos Solitons Fractals **143**, 110551 (2021)
14. Sakkaravarthi, K., Kanna, T., Mareeswaran, R.B.: Higher-order optical rogue waves in spatially inhomogeneous multimode fiber. Phys. D **435**, 133285 (2022)
15. Jia, H.P., Bin, Li., Yang, R.C., Tian, J.P.: Diverse composite waves in coherently coupled inhomogeneous fiber systems with external potentials. Nonlinear Dyn. **99**, 2987–2999 (2020)
16. Mahato, D.K., Govindarajan, A., Lakshmanan, M., Sarma, A.K.: Dispersion managed generation of Peregrine solitons and Kuznetsov-Ma breather in an optical fiber. Phys. Lett. A **392**, 127134 (2021)
17. Nandy, S., Barthakur, A.: Dark-bright soliton interactions in coupled nonautonomous nonlinear Schrödinger equation with complex potentials. Chaos Solitons Fractals **143**, 110560 (2021)
18. Xiong, G., He, J.R., Wang, K.W., Xue, L.: Analytical light bullet solutions in diffraction-decreasing media with inhomogeneous parameters. Results Phys. **43**, 106111 (2022)
19. He, J.R., Deng, W.W., Xue, L.: Snakelike similaritons in combined harmonic-lattice potentials with a varying source. Nonlinear Dyn. **100**, 1599–1609 (2020)
20. Kanna, T., Sheela, A.A., Mareeswaran, R.B.: Spatially modulated two- and three-component Rabi-coupled Gross-Pitaevskii systems. J. Phys. A Math. Theor. **52**, 375201 (2019)
21. Djoptoussia, C., Tiofack, C.G.L., Alim, Mohamadou, A., Kofané, T.C.: Ultrashort self-similar periodic waves and similaritons in an inhomogeneous optical medium with an external source and modulated coefficients. Nonlinear Dyn. **107**, 3833–3846 (2022)
22. Liu, X.Y., Zeng, J.H.: Overcoming the snaking instability and nucleation of dark solitons innonlinear Kerr media by spatially inhomogeneous defocusing nonlinearity. Chaos Solitons Fractals **156**, 111803 (2022)
23. López, R.C., Sun, G.H., Camacho-Nieto, O., Yáñez-Márquez, C., Dong, S.H.: Analytical traveling-wave solutions to a generalized Gross-Pitaevskii equation with some new time and space varying nonlinearity coefficients and external fields. Phys. Lett. A **381**, 2978–2985 (2017)
24. Liu, C., Yang, Z.Y., Zhao, L.C., Xin, G.G., Yang, W.L.: Optical rogue waves generated on Gaussian background beam. Opt. Lett. **39**(4), 1057 (2014)
25. Kundu, N., Ghosh, S., Roy, U.: Quantum simulation of rogue waves in Bose-Einstein condensate: an exact analytical method. Phys. Lett. A **449**, 128335 (2022)
26. Liu, C., Chen, S.C., Yao, X.K., Akhmediev, N.: Non-degenerate multi-rogue waves and easy ways of their excitation. Phys. D **433**, 133192 (2022)
27. Wang, Y.Y., Chen, L., Dai, C.Q., Zheng, J., Fan, Y.: Exact vector multipole and vortex solitons in the media with spatially modulated cubic-quintic nonlinearity. Nonlinear Dyn. **90**, 1269–1275 (2017)
28. Zhong, W.P., Belic, M., Malomed, B.A.: Rogue waves in a two-component Manakov system with variable coefficients and an external potential. Phys. Rev. E **92**, 053201 (2015)
29. Gromova, E.M., Malomed, B.A., Tyutin, V.V.: Vector solitons in coupled nonlinear Schrödinger equations with spatial stimulated scattering and inhomogeneous dispersion. Commun. Nonlinear Sci. **54**, 13–20 (2018)
30. Chen, Y.X.: Vector peregrine composites on the periodic background in spin–orbit coupled Spin-1 Bose-Einstein condensates. Chaos Solitons Fractals **169**, 113251 (2023)
31. Zhong, W.P., Chen, L., Belic, M., Petrovic, N.: Controllable parabolic-cylinder optical rogue wave. Phys. Rev. E **90**, 043201 (2014)
32. He, J.R., Li, H.M.: Analytical solitary-wave solutions of the generalized nonautonomous cubic-quintic nonlinear

Schrödinger equation with different external potentials. Phys. Rev. E **83**, 066607 (2011)
33. Wang, S.J., Liu, B., Hu, M.L., Wang, C.Y.: On the efficiency of parabolic self-similar pulse evolution in fiber amplifiers with gain shaping. J. Lightwave Technol. **34**(13), 3023–3034 (2016)
34. Tegin, U., Kakkava, E., Rahmani, B., Psaltis, D., Moser, C.: Spatiotemporal self-similar fiber laser. Optica **6**(11), 1412–1415 (2019)
35. Tiofack, C.G.L., Coulibaly, S., Taki, M., Bièvre, S.D., Dujardin, G.: Kuznetsov-Ma soliton formation in nonlinear Schrödinger equations. Phys. Lett. A **381**, 1999–2003 (2017)
36. Yang, Z.P., Zhong, W.P., Belic, M., Zhang, Y.Q.: Controllable optical rogue waves via nonlinearity management. Opt. Express **26**(6), 7587 (2018)
37. Duan, L., Yang, Z.Y., Liu, C., Yang, W.L.: Optical rogue wave excitation and modulation on a bright soliton background. Chin. Phys. Lett. **33**(1), 010501 (2016)
38. Wang, M., Tian, B.: In an inhomogeneous multicomponent optical fiber: Lax pair, generalized Darboux transformation and vector breathers for a three-coupled variable-coefficient nonlinear Schrödinger system. Eur. Phys. J. Plus. **136**, 1002 (2021)
39. Zhong, W.P., Yang, Z.P., Belic, M., Zhong, W.Y.: Controllable optical rogue waves in inhomogeneous media. Phys. Lett. A **453**, 128469 (2022)
40. Gorza, S.P., Kockaert, P., Emplit, P., Haelterman, M.: Oscillatory neck instability of spatial bright solitons in hyperbolic systems. Phys. Rev. Lett. **102**, 134101 (2009)
41. Erkintalo, M., Hammani, K., Kibler, B., Finot, C., Akhmediev, N., Dudley, J.M., Genty, G.: Higher-order modulation instability in nonlinear fiber optics. Phys. Rev. Lett. **107**, 253901 (2011)
42. Bailung, H., Sharma, S.K., Nakamura, Y.: Observation of Peregrine solitons in a multicomponent plasma with negative ions. Phys. Rev. Lett. **107**, 255005 (2011)
43. Steer, J.N., Borthwick, A.G.L., Onorato, M., Chabchoub, A., Bremer, T.S.V.D.: Hydrodynamic X waves. Phys. Rev. Lett. **123**, 184501 (2019)
44. He, Y.C., Slunyaev, A., Mori, N., Chabchoub, A.: Experimental evidence of nonlinear focusing in standing water waves. Phys. Rev. Lett. **129**, 144502 (2022)
45. Chabchoub, A., Hoffmann, N., Onorato, M., Slunyaev, A., Sergeeva, A., Pelinovsky, E., Akhmediev, N.: Observation of a hierarchy of up to fifth-order rogue waves in a water tank. Phys. Rev. E **86**, 056601 (2012)
46. Hnat, B., Kolotkov, D.Y., Connell, D.O., Nakariakov, V.M., Rowlands, G.: Nonlinear waves in the terrestrial quasiparallel foreshock. Phys. Rev. Lett. **117**, 235102 (2016)
47. Tiofack, C.G.L., Coulibaly, S., Tak, M., Bievre, S.D., Dujardin, G.: Comb generation using multiple compression points of Peregrine rogue waves in periodically modulated nonlinear Schrödinger equations. Phys. Rev. A **92**, 043837 (2015)
48. Guo, L.H., Chen, P., Tian, J.S.: Peregrine combs and rogue waves on a bright soliton background. Optik **227**, 165455 (2021)
49. Kruglov, V.I., Triki, H.: Periodic and solitary waves generating in optical fiber amplifiers and fiber lasers with distributed parameters. Phys. Lett. A **461**, 128644 (2023)
50. Agrawal, G.P.: Nonlinear Fiber Optics, 4th edn. Academic Press, New York (2007)
51. Chabchoub, A., Hoffmann, N.P., Akhmediev, N.: Rogue wave observation in a water wave tank. Phys. Rev. Lett. **106**(20), 204502 (2011)
52. Chabchoub, A., Hoffmann, N., Onorato, M., Akhmediev, N.: Super rogue waves: observation of a higher-order breather in water waves. Phys. Rev. X **2**(1), 011015 (2012)
53. Yang, D.Y., Tian, B., Tian, H.Y., Wei, C.C., Shan, W.R., Jiang, Y.: Darboux transformation, localized waves and conservation laws for an M-coupled variable-coefficient nonlinear Schrödinger system in an inhomogeneous optical fiber. Chaos Solitons Fractals **156**, 111719 (2022)
54. Chakraborty, S., Nandy, S., Barthakur, A.: Bilinearization of the generalized coupled nonlinear Schrödinger equation with variable coefficients and gain and dark-bright pair soliton solutions. Phys. Rev. E **91**, 023210 (2015)
55. Nandy, S., Barthakur, A.: Pairwise three soliton interactions, soliton logic gates in coupled nonlinear Schrödinger equation with variable coefficients. Commun. Nonlinear Sci. **69**, 370–385 (2019)
56. Cai, J.X., Bai, C.Z., Zhang, H.H.: Decoupled local/global energy-preserving schemes for the N-coupled nonlinear Schrödinger equations. J. Comput. Phys. **374**, 281–299 (2018)
57. Qin, Y.H., Zhao, L.C., Yang, Z.Y., Yang, W.L.: Several localized waves induced by linear interference between a nonlinear plane wave and bright solitons. Chaos **28**, 013111 (2018)
58. Solli, D.R., Ropers, C., Koonath, P., Jalali, B.: Optical rogue waves. Nature **450**, 1054 (2007)